2020 19th IEEE International Conference on Machine Learning and Applications (ICMLA) | 978-1-7281-8470-8/20/$31.00 ©2020 IEEE | DOI: 10.1109/ICMLA51294.2020.00109

Distance-Based Multivariate Anomaly Detection in Wire Arc Additive Manufacturing

Raven Reisch*†, Tobias Hauser†, Benjamin Lutz†, Matteo Pantano†, Tobias Kamps† and Alois Knoll*
*Chair of Robotics, Artificial Intelligence and Real-time Systems
Technical University of Munich (TUM), Munich, Germany
Email: raven.reisch@tum.de, knoll@mytum.de
†Siemens AG, Munich, Germany
Email: {raven.reisch, tobias.hauser, lutz.benjamin, matteo.pantano, tobias.kamps}@siemens.com

***Abstract*—Wire Arc Additive Manufacturing (WAAM) offers the possibility to build up large-scale metal parts. Data which is obtained from a multivariate sensor system in-situ must be analyzed automatically to ensure an early and reliable detection of defects to reduce the costs due to production scrap. For that reason, a modular anomaly detector for multivariate time series in WAAM was investigated in this paper. The approach adressed major topics in real-life data sets of industrial applications such as miscellaneous signal sample rates, lack of synchronization and concept drift. A reference data set based on an anomaly-dependently splitted time horizon was defined to reduce the sensitivity loss of the detector after an anomaly. To avoid the need for labeled data, an unsupervised anomaly detection method based on neural networks was used. Hence, no time and costs for artificial defect creation on the machine tool are required when implementing the approach in industrial applications.**

***Keywords*-Anomaly Detection, Time Series, Multivariate, Additive Manufacturing, Machine Learning**

I. Introduction

Anomaly detection represents an emerging topic in digital manufacturing [1]. Defects must be detected within a short period of time to ensure a safe and secure operation of costly production machines and a high quality of the outcome to prevent costs due to increased maintenance, preventable downtime, and avoidable production scrap [2].
In particular, for additive manufacturing (AM), defect detection based on process monitoring data allows to detect part internal defects as the build-up procedure is conducted layer upon layer. Especially for large-scale parts, hereby, costly and complicated non-destructive testing after the production can be avoided [3]. An AM technology for the production of large-scale metal parts is arc welding based Wire Arc Additive Manufacturing (WAAM). Here, the Cold Metal Transfer (CMT) process is commonly used, as it allows low heat input and thus, lower residual stresses caused by heat [4]. Potential defects in WAAM are among others oxidation, lack of fusion and form deviations. To detect these defects in WAAM, this study introduces a framework for defect detection based on a context-sensitive unsupervised anomaly detection method for multivariate time series. The main contributions of this article are the following:

- The architecture of a statistic approach for anomaly detection in multivariate data streams in the scope of industrial applications is introduced.
- Time series with different sample rates and concept drift are addressed by defining a time horizon as reference. The time horizon can be divided to prevent lower detection sensitivity after an occurred anomaly.
- The proposed approach is validated using a real-life data set acquired in the WAAM process.
- Three types of neural networks are presented as prediction and evaluation models of the anomaly detection framework. Upon applying a dimensional reduction on image data, data fusion is conducted by calculating an anomaly score which is representing the probability of a defect.

The remainder of this article is structured as follows. In Section II, technical terms are introduced. In Section III, related work in the area of anomaly detection in time series is presented. Section IV reveals the architecture of the statistic approach. Section V is dedicated to the experimental implementation and validation in the industrial WAAM use case. In Section VI, the results are discussed and Section VII summarizes the work.

II. Definitions

In this paper, the definitions for the following technical terms are considered:

- **Time Series**: Time series appear as sequencial data [5]. Hence, a time series $\vec{T}$ is a temporally ordered set of n variables with i as the index of the latest value as noted in equation 1 [6].

$$\vec{T} = t[i], ..., t[i-n] \tag{1}$$

- **Anomaly**: Anomalies are indicated by an abnormal behaviour compared to the normal behaviour. The term *outlier* is often used as synonym for anomalous data. By definition, anomalies occur rarely. [5], [7]
- **Concept Drift**: Concept drift occurs when the normal system behavior changes over time [8].

978-1-7281-8470-8/20/$31.00 ©2020 IEEE
DOI 10.1109/ICMLA51294.2020.00109

III. Related work

Anomaly detection can be conducted supervised, semi-supervised, or unsupervised [5].

For supervised methods, anomaly labels must be available. Here, the imbalance in the data set due to the rareness of anomalies must be considered [5], [7]. Rule-based systems are created by transferring previously defined characteristics of labeled anomalies into rules to detect outliers with the same characteristics in new data sets [8].

In the semi-supervised case, training data includes labeled normal behavior. Detection models rise an alarm when data patterns do not fit to the normal behavior. Salvador et al. introduced such an approach for a rule-based anomaly detector [9]. Ahrens et al. proposed a distance-based approach by searching for similarities in the normalized data. [10]

(Semi-)Supervised techniques are often unsuitable for real-world applications as anomalies are often neither labeled nor completely known [11]. By contrast, unsupervised methods benefit from the defined rareness of anomalies by considering the corpus of data as normal [5]. Techniques such as thresholding, exponential smoothing [12], unsupervised clustering [13] or change point detection methods [14] are used. Malhotra et al. presented a Long Short Term Memory (LSTM) model to detect anomalies in data of a Space Shuttle valve [15]. Chauhan et al. used LSTMs for anomaly detection in medical data of an electrocardiogram [16]. Yen et. al. proposed a method based on convolutional LSTMs to decrease the reduction in accuracy due to concept drift in computer system logging data [8]. Jin et al. presented a convolutional neural network to detect anomalies in sequential infrared images with synthetic anomalies [17]. Ahmad et al. suggested the use of an hierarchical temporal memory (HTM) and calculated the likelihood of anomalies based on the difference between the predicted and the real data. By including a Gaussian convolutional kernel, not perfectly synchronized multivariate time series were combined. [18]

In the application of AM, research in anomaly detection focuses on the technology of laser powder bed fusion and fused deposition modeling [19]. For WAAM, anomaly detection was conducted on the data of multiple sensors such as current [20], acoustic [21] and thermal [22] emissions as well as on the visual appearance of the weld bead [23], [24]. Chen et al. fused multi-sensor data in welding processes by using a fuzzy integral method [25].

IV. Anomaly Detection Framework

In industrial use cases, the artificial creation of data containing defects is costly and time-consuming and therefore unwanted. Hence, the shortage of labeled anomalies is evident. However, a large data set for mostly normal system behavior is usually available. For that reason, unsupervised anomaly detection methods are a valid choice for industrial use cases as no previously labeled data is needed. In this study, a modular unsupervised anomaly detection method for multivariate time-series $\overrightarrow{T_q}$ with $q = 1, ..., k$ was investigated. First, unsupervised trained models were used to predict the consecutive time step $x_{pred,q}$. Then, the reconstruction error ed_q was calculated. The error stream served as input to a likelihood estimation algorithm which generated an anomaly score D_M. D_M was determined using a reference data set which was adjusted depending on the information from the feedback loop. The anomaly score was then used as indicator for defects t_{annot} in the process. The modular approach is shown in Figure 1 and detailed in the following subsections.

A. Prediction models

Each sensor creates a time series $\vec{T}_q$ with a sample rate f_q. The values are normalized in real-time based on the measuring range of the sensor. The signal $\vec{T}_q = t_q[i], ..., t_q[i-n]$ of sensor q serves as input to a signal specific prediction model such as ARIMA or a neural network. The training is based on an unlabeled initial data set. The prediction model must be chosen accordingly to consider different scenarios such as periodic patterns. The output of each model is a stream of predictions $\vec{x}_{pred,q}[i, ..., i-n]$ which represent the expected subsequent values.

B. Error distances

The predicted values are compared to the values of the real signal $t_q[i]$. The error is calculated by equation (2) and is called error distance $ed_q[i]$ in the following. To calculate the error distance for multidimensional data such as images, the root mean square error along the pixel matrix is chosen, indicating the cumulated deviations between the pixels of the real and the reconstructed images. Hereby, the error distance conducts the dimensional reduction and for instances, reduces an image to a scalar value.

$$ed_q[i] = t_q[i] - x_{pred,q}[i] \tag{2}$$

Depending on the characteristics of the input data, a convolutional kernel can be applied on the resulting error distance streams to realize a moving average or a Gaussian filter. Hereby, noise is filtered and minor synchronization differences between various time series are balanced. An averaging kernel also increases the chance of correlating anomalous peaks with minor delays in different time series. With each time step, a new error distance is calculated, resulting in an error distance stream $\overrightarrow{ed_q}$ for each signal. Depending on the chosen prediction model, concept drift can result in an increase of the error distance.

C. Anomaly score

To conduct the outlier detection, a Bregman distance between the current data point and a reference data set is calculated. Therefore, the statistical distributions for the past error distances of all signals are considered by implementing

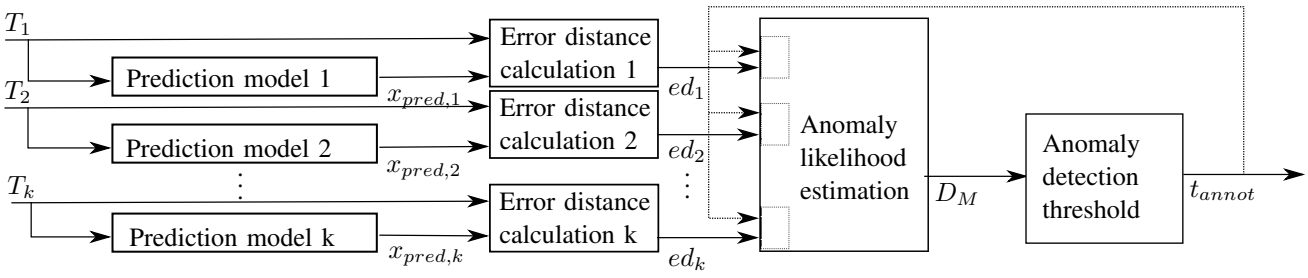

Figure 1. Approach of the proposed multivariate anomaly detector

the Mahalanobis Distance D_M of equation (3). The Mahalanobis Distance is scalar invariant and thus, can be used for data streams with different scales.

$$D_M(x) = \sqrt{(\vec{ed}[i] - \vec{\mu})^T * S^{-1} * (\vec{ed}[i] - \vec{\mu})} \quad (3)$$

As part of this distance, the covariance matrix S as well as the vector $\vec{\mu}$ with the means μ_q of the k error distance streams is needed. In case of online monitoring, these variables depend on m time steps in the past. As not all sensors necessarily offer the same sample rate, m is adapted to each time series individually. For that reason, a time horizon H_T which depicts a reference data set for the calculation of D_M is defined. When no concept drift exists or it has already been included in the initial data set, H_T can be based on the validation part of the initial data set. Otherwise, H_T is created based on a sliding window with a predefined offset o to the latest time step i. To allow online monitoring, the choice of o must comply to equation 4.

$$o > 0 \quad (4)$$

The choice of H_T defines the ground truth for the anomaly detection and influences the sensitivity of the detector. Without any changes, anomalies affect the sensitivity of the following time steps. To face this problem, the time horizon is divided into w parts as shown in Figure 2 by p_1 and p_2 and as noted in equation (5). As only past data without anomalous behavior are considered, H_T does not contain anomalies. The information about the anomalous behavior is obtained by a feedback loop (see Figure 1) which provides information of the final anomaly evaluation for past time steps. Hereby, a reduction of the sensitivity after an anomaly is prevented and long-term anomalies such as machine failures can also be detected reliable.

$$H_T = p_1 + ... + p_w \quad (5)$$

For a known sample rate f_q, the signal specific number of time steps m_q is calculated by equation (6).

$$m_q = H_T * f_q \quad (6)$$

Based on H_T, $\vec{\mu}$ and S are calculated by equations (7), (8), (9) and (10) with $r = 1, ..., k$ and $s = 1, ..., k$.

$$\mu_q = \frac{1}{m_q} * \sum_{j=1}^{m_q} ed_q[i-j] \quad (7)$$

$$\sigma_{rr}^2 = \frac{1}{m_r - 1} * \sum_{j=1}^{m_r} (ed_r[i-j] - \mu_r)^2 \quad (8)$$

$$\sigma_{rs}^2 = \frac{1}{m_r - 1} * \sum_{j=1}^{m_r} (ed_r[i-j] - \mu_r) * (ed_s[i-j] - \mu_s) \quad (9)$$

$$S = (\vec{ed}[i] - \vec{\mu}[i]) * (\vec{ed}[i] - \vec{\mu}[i])^T = \begin{pmatrix} \sigma_{1,1}^2 & a_{1,2} & \cdots & a_{1,s} \\ a_{2,1} & \sigma_{2,2}^2 & \cdots & a_{2,s} \\ \vdots & \vdots & \ddots & \vdots \\ a_{r,1} & a_{r,2} & \cdots & \sigma_{r,s}^2 \end{pmatrix} \quad (10)$$

D_M is an indicator for the predictability of the data. If the data is less predictable, an anomaly is more probable. By introducing a sliding window as reference, a constant increase of the error distance due to concept drift only has minor effects on the anomaly detection itself. However, if the models are sensitive to concept drift, retraining must be initialized. A model change can be avoided by implementing self-adaptable models or continuous learning.

D. Detection threshold

A threshold filter is applied on the anomaly score to detect defects. Here, a conflict of objective between the optimization of classification accuracy for normal data and the chance of misclassifying abnormal data is present. The

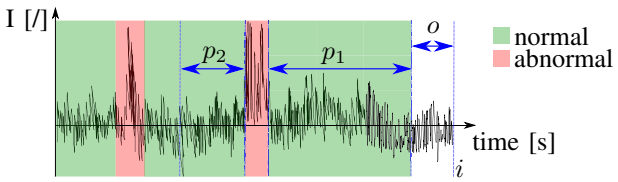

Figure 2. Example of a divided time horizon H_T into p_1 and p_2 and offset o from the latest time step i

threshold is defined as maximum anomaly score in the test data of the initial data set. Alternatively, an adaptive threshold based on the sum of mean and standard deviation of the reference data set can be introduced.

V. Implementation in Wire Arc Additive Manufacturing

As described in [26], an electrical sensor provided synchronized current and voltage data of the WAAM process with a sample rate of 3200 Hz. Optical data of the region of deposition were provided by an 8-bit gray-scale welding camera with a sample rate of 50 Hz.
Three types of defects were created along the build-up procedure by forcing either an oxidation due to a reduced inert gas flow, a lack of fusion due to a polluted substrate and form deviations in the build-up process because of insufficient material deposition in the previous layer. These defects resulted in anomalies in the time series and were meant to be detected by the proposed approach. The signals were normalized by the measuring area of each sensor.

A. Prediction models

The time series were analyzed by three types of machine learning models to emphasize the modular concept.

1) Current prediction: The current and voltage data showed repetitive patterns. Deviations from these patterns indicated an anomalous behaviour. A neural network with LSTMs was used to predict the current data. The model structure as well as the hyperparameters were optimized with a Bayesian Hyperparameter Optimization (HPO), resulting in a model architecture consisting out of two layers with 68 LSTM cells each and one fully-connected layer with ReLU activation function and the hyperparameter set in Table I. The unlabeled training data comprised 60000 time steps

Table I
Hyperparameters of machine learning models

Parameter	***LSTM model***	***Conv1D model***	***Autoencoder***
Input time steps	33	348	1
Output time steps	1	1	1
Batch size	71	20	20
Optimizer	Adam	Adam	RMSprop
Learning rate	1.8 e-04	1.4 e-04	1 e-03
Dropout	9.5 e-04	1.1 e-01	None
Epochs	50	100	10

of a previous additive layer without forced anomalies. The current time series as well as its prediction and the resulting error are illustrated in Figure 3. Three CMT cycles can be seen. For the first cycle, the model fitted well to the data. The following two cycles had a slightly different duration and thus, the predicted values did not fit perfectly to the real data, especially in case of high gradients. A root mean square error (rmse) of $rmse_{LSTM} = 9.00e{-}3$ was achieved with test data.

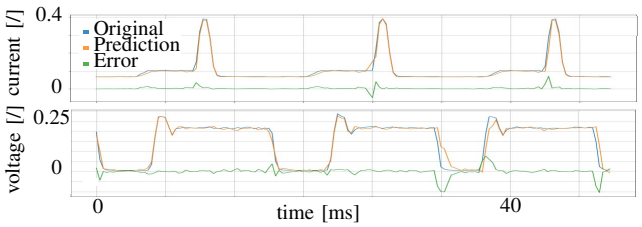

Figure 3. Normalized not synchronized current and voltage time series (blue), their predictions (orange) and the resulting error distances (green)

2) Voltage prediction: To predict the voltage data, a model based on one-dimensional convolutional (Conv1D) elements was chosen, optimized by a Bayesian HPO and trained on the voltage data with the same time period as the LSTM model. The final model architecture consisted of five layers with a Conv1D layer as input layer and a fully connected layer with ReLU activation function as output layer. The hyperparameters can be seen in Table I. Three CMT cycles of the voltage data as well as their predictions and the resulting error distances are illustrated in Figure 3. The prediction in the first cycle fitted well while deviations between the real values and the predicted ones arised in the areas of higher gradients in the following two cycles. A rmse of $rmse_{Conv1D} = 10.11e - 3$ was achieved.

3) Video evaluation: The video data was evaluated with an autoencoder. Hence, instead of a prediction, an image reconstruction was accomplished. The size of the input data, showcased by the upper six images in Figure 4, was reduced to 200x300 pixels to decrease the computational complexity of the task. The autoencoder consisted of an encoder-decoder structure with eight layers each. The encoder and decoder part included six convolutional 2D layers and two max pooling respectively up sampling layers. The chosen hyperparameters can be seen in Table I. In Figure 4, a comparison of original images of the normal (a,d,e,f) and abnormal (b,c) process with the reconstructed images is shown. The reconstructed images fitted well in case of normal behavior. When an anomaly occurred, the autoencoder had to deal with unlearned details, resulting in a worse fit.

B. Error distance

In Figure 5, the error distances for three additive layers are shown. An averaging kernel with a window length of 64 was applied on the error distances of current and voltage for synchronization. Hereby, anomalous peaks in the error distances of the electrical data were correlated to peaks in the error distance of the images despite having minor delays in the data acquisition. In layer 1 (blue) oxidation took places. This anomaly was visible in all error distances. Same can be concluded for layer 2 (red). Here, the oxidation of the previous layer resulted in further anomalies. In layer 3

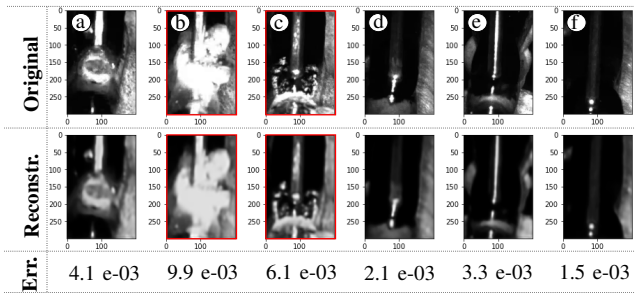

Figure 4. Original/Reconstructed images of welding camera and corresponding reconstruction error; images of abnormal process marked in red

(green) a form deviation was included. The anomaly was seen in the error distances of current and voltage, but hardly in the one of the images. The numbers along the error distances of the video stream indicate the time step of the image and correspond to the numbers in Figure 4.

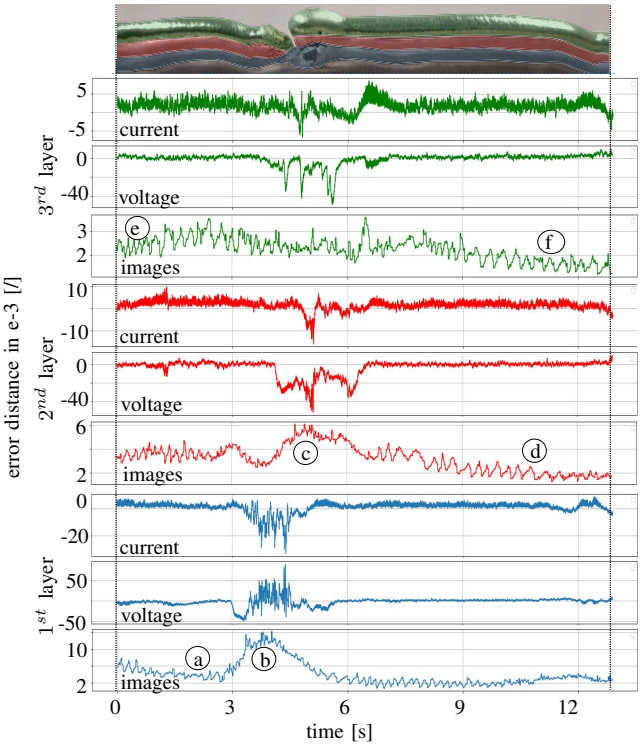

Figure 5. WAAM wall with forced anomalies (oxidation in layer 1 (blue), polluted surface in layer 2 (red), form deviation in layer 3 (green)) and correlating error distances of the time series for current, voltage, and the welding camera; circled annotations correspond to the images in Figure 4

C. Anomaly Score and Anomaly Threshold

Data fusion was conducted by implementing the methods of section IV-C. In Figure 6, D_M as well as a threshold are illustrated for the three layers. The anomalous behavior

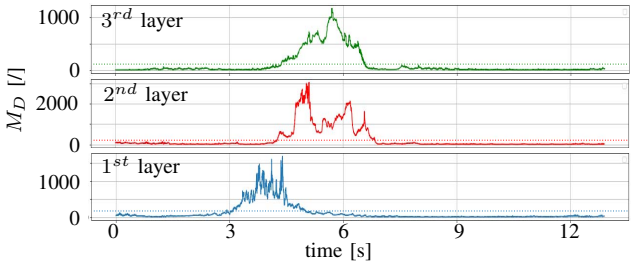

Figure 6. Mahalanobis Distance of three layers of a wall which was manufactured by WAAM with forced anomalies

is evident. The defects were unambiguously identified by implementing the threshold filter. False positives or false negatives were removed by adjusting the threshold and changing H_T to receive a higher or lower sensitivity of the anomaly detector. Adjustments of the threshold also influenced the splits of H_T as mentioned in Section IV-C.

VI. Discussion

The proposed approach detects defects due to oxidation, polluted surfaces and form deviations in industrial WAAM data. The anomaly score in Figure 6 showed a good match with the real defects. However, also the error distances have a strong correlation to the real defects even without computing the likelihood of the event. Hence, it can be stated that the LSTM and Conv1D models are a valid choice for the proposed application. In the third layer, the image error distance showed only minor deviations in case of a defect in comparison to the ones of the electrical data. By taking a closer look on the error distances of the voltage and the current, the voltage error distance offered the most obvious peaks in case of anomalies. Both models showed a similar loss of $rmse_{LSTM}$ and $rmse_{Conv1d}$ for the test data set. The autoencoder had the lowest loss even if the model was trained for only 10 epochs. Due to the higher complexity, the prediction time per time step of the LSTM model was slightly higher than the one of the Conv1D model as noted in Table II. The prediction time of the autoencoder surpasses both by a factor of 10 because of the higher dimensionality of the input data. The prediction time can be further reduced by either decreasing the model complexity to reduce the computational requirements for model execution or by increasing the computational performance of the hardware. In industrial environments, the computational performance can be increased by using edge computing.

Table II
Characteristics of the Machine Learning Models

	LSTM	***Conv1D***	***Autoencoder***
Loss (rmse)	9.00 e-3	10.11 e-3	1.98 e-3
Prediction time per instance	29.2 ms	23.4 ms	340.8 ms

To receive the shown results, extensive hyperparameter tuning was needed. For instance, a Bayesian HPO was conducted to obtain the model parameters. In addition, parameters such as H_T must be set manually. The sensitivity of the detector highly depends on the right choice of these values. However, as soon as the right parameters are defined, concept drift can be addressed as minor inaccuracies of the initial models are compensated. In WAAM, concept drift occurs for the voltage data due to a changed inert gas flow. In the presented data, concept drift occurred after the oxidation had been forced as a higher inert gas flow was reached, resulting in a different voltage level and hence, a worse fit of the prediction model with an increased rmse of $rmse_{Conv1D-Drift} = 13.97e-03$. However, anomaly detection based on the initial model was still possible, indicating a low sensitivity in case of concept drift.

In many applications, the combination of several time series improves the anomaly detection. In WAAM, the voltage time series provides enough information to detect many anomalies. However, the combination with current and camera data is needed to obtain additional information about the anomaly, to introduce redundancy into the monitoring system and to increase detection reliability. To detect additional anomalies such as pores and to evaluate the robustness of the approach, further research must be conducted.

VII. Conclusion

In this study, a modular, unsupervised anomaly detection approach for multivariate time series data was investigated. It was based on the Mahalanobis distance and adressed major topics in real-life data sets of industrial applications such as miscellaneous signal sample rates, lack of synchronization, and concept drift. To avoid a reduced sensitivity of the detector system after an anomaly occurs, a dynamic reference data set based on an anomaly dependently splitted time horizon was defined. The proposed approach was validated on industrial WAAM data and showed the capability of detecting anomalies due to oxidation, form deviations as well as polluted surfaces. Prediction models based on LSTMs and Conv1D cells as well as an autoencoder were chosen and verified as valid choice.

Acknowledgment

The authors gratefully acknowledge funding from EIT RawMaterials for the project SAMOA - Sustainable Aluminium additive Manufacturing fOr high performance Applications, no. 18079.

References

[1] M. Haselmann, D. P. Gruber, and P. Tabatabai, "Anomaly detection using deep learning based image completion," *ICMLA*, 2018.

[2] B. Lutz, D. Kisskalt, D. Regulin, R. Reisch, A. Schiffler, and J. Franke, "Evaluation of deep learning for semantic image segmentation in tool condition monitoring," *ICMLA*, pp. 2008–2013, 2019.

[3] T. A. Rodrigues, V. Duarte, R. M. Miranda, T. G. Santos, and J. P. Oliveira, "Current status and perspectives on wire and arc additive manufacturing (waam)," *Materials (Basel, Switzerland)*, vol. 12, no. 7, 2019.

[4] S. Selvi, A. Vishvaksenan, and E. Rajasekar, "Cold metal transfer (cmt) technology - an overview," *Defence Technology*, vol. 14, no. 1, pp. 28–44, 2018.

[5] V. Chandola, A. Banerjee, and V. Kumar, "Anomaly detection: A survey," *ACM Computing Surveys*, vol. 41, no. 3, 2009.

[6] E. Keogh, J. Lin, and A. Fu, "Hot sax: Efficiently finding the most unusual time series subsequence," in *ICDM*. IEEE Computer Society Press, 2005, pp. 226–233.

[7] R. Chalapathy and S. Chawla, "Deep learning for anomaly detection: A survey," 2019.

[8] S. Yen, M. Moh, and T.-S. Moh, "Causalconvlstm: Semi-supervised log anomaly detection through sequence modeling," *ICMLA*, 2019.

[9] S. Salvador and P. Chan, "Learning states and rules for detecting anomalies in time series," *Applied Intelligence*, vol. 23, no. 3, pp. 241–255, 2005.

[10] L. Ahrens, J. Ahrens, and H. D. Schotten, "A machine-learning phase classification scheme for anomaly detection in signals with periodic characteristics," *EURASIP Journal on Advances in Signal Processing*, no. 1, p. 507, 2019.

[11] N. Goernitz, M. M. Kloft, K. Rieck, and U. Brefeld, "Toward supervised anomaly detection," *Journal of Artificial Intelligence Research*, vol. 46, pp. 235–262, 2013.

[12] M. Szmit and A. Szmit, "Usage of modified holt-winters method in the anomaly detection of network traffic: Case studies," *Journal of Computer Networks and Communications*, vol. 2012, pp. 1–5, 2012.

[13] V. Saligrama and Z. Chen, "Video anomaly detection based on local statistical aggregates," pp. 2112–2119, 2012.

[14] R. P. Adams and D. J. C. MacKay, "Bayesian online changepoint detection," 2007.

[15] P. Malhotra, L. Vig, G. Shroff, Agarwal, and A. Puneet, "Long short term memory networks for anomaly detection in time series," *ESANN 2015 proceedings, European Symposium on Artificial Neural Networks, Computational Intelligence*, 2015.

[16] S. Chauhan and L. Vig, "Anomaly detection in ecg time signals via deep long short-term memory networks," pp. 1–7, 2015.

[17] B. Jin, Y. Tan, A. Nettekoven, Y. Chen, U. Topcu, Y. Yue, and A. Sangiovanni-Vincentelli, "An encoder-decoder based approach for anomaly detection with application in additive manufacturing," *ICMLA*, 2019.

[18] S. Ahmad and S. Purdy, "Real-time anomaly detection for streaming analytics," 2016.

[19] X. Qi, G. Chen, Y. Li, X. Cheng, and C. Li, "Applying neural-network-based machine learning to additive manufacturing: Current applications, challenges, and future perspectives," *Engineering*, vol. 5, no. 4, pp. 721–729, 2019.

[20] A. Mazlan, H. Daniyal, A. I. Mohamed, M. Ishak, and A. A. Hadi, "Monitoring the quality of welding based on welding current and ste analysis," *IOP Conference Series: Materials Science and Engineering*, vol. 257, 2017.

[21] M. Cudina, J. Prezelj, and I. Polajnar, "Use of audible sound for on-line monitoring of gas metal arc welding process," *Metalurgija -Sisak then Zagreb*, pp. 81–85, 2008.

[22] D. Yang, G. Wang, and G. Zhang, "Thermal analysis for single-pass multi-layer gmaw based additive manufacturing using infrared thermography," *Journal of Materials Processing Technology*, vol. 244, pp. 215–224, 2017.

[23] M. Purrio, "Prozessanalyse und -überwachung beim metallschutzgasschweißen durch optische in-situ-sensorsysteme: Process analysis and monitoring in gas metal arc welding by optical in-situ sensor systems," Aachen, 2017.

[24] T. Hauser, A. D. Silva, R. T. Reisch, J. Volpp, T. Kamps, and A. F. Kaplan, "Fluctuation effects in wire arc additive manufacturing of aluminium analysed by high-speed imaging," *Journal of Manufacturing Processes*, vol. 56, 2020.

[25] B. Chen, S. Chen, and J. Feng, "A study of multisensor information fusion in welding process by using fuzzy integral method," *The International Journal of Advanced Manufacturing Technology*, vol. 74, no. 1-4, pp. 413–422, 2014.

[26] R. Reisch, T. Hauser, T. Kamps, and A. Knoll, "Robot based wire-arc-additive-manufacturing system with context-sensitive multivariate monitoring framework," *FAIM*, 2020.